Autoproteolysis of Rat p67 Generates Several Peptide Fragments: The N-Terminal Fragment, p26, Is Required for the Protection of eIF2α from Phosphorylation†

Bansidhar Datta,* Arnab Ghosh, Avijit Majumdar, and Rekha Datta

Department of Chemistry, Kent State University, Kent, Ohio 44242

Received September 2, 2006; Revised Manuscript Received January 5, 2007

ABSTRACT: Eukaryotic initiation factor 2-associated glycoprotein, p67, plays important roles in the regulation of eIF2α phosphorylation and thus maintains cell growth and proliferation. The p67 sequence can be divided into two segments, the N-terminal segment of amino acids 1−107 (p26) and the downstream segment of amino acids 108−480 (p52). Comparison of the amino acid sequences of p67 from lower to higher organisms suggests that there is a progressive addition of several unique domains at the N-terminus of p67, and these unique domains, which are present in p26, play important roles in the modulation of eIF2α phosphorylation in mammalian cells. To test the hypothesis that the p26 segment is generated from p67 due to its autoproteolysis and whether p26 is required for the protection of eIF2α from phosphorylation, we have analyzed the time-dependent cleavage of functionally active rat recombinant p67 purified from either baculovirus-infected insect cells or transiently transfected mammalian cells. We noticed a regulated cleavage of p67 that generates several peptides along with the most stable p26 and p52 fragments. The p52 fragment has a low level of autoproteolysis activity that possibly increases the autoproteolysis of full-length p67. This activity could not be inhibited by a serine protease inhibitor, PMSF, but could be inhibited by a cocktail of protease inhibitors that includes bestatin, leupeptin, E64, AEBSF, and aprotinin. To provide evidence that the fragmentation of p67 is not due to the presence of any contaminant protease(s), we fractionated purified rat p67 with molecular sieve, anion exchange, and cation exchange chromatographic steps performed in the presence of different K^+ ion concentrations. Our data show that the extent of cleavage of p67 into different fragments is higher in the presence of 0.75 M K^+ ion and in samples stored at −80 °C. Under parallel conditions, p67's mutants, D251A and D262A, exhibited very little to no cleavage, whereas the H231E mutant exhibited extensive cleavage that generated a large amount of p26 fragment. The p26 fragment exhibited protection of eIF2α phosphorylation both in vivo and in vitro. Altogether, our data provide evidence that rat p67 has autoproteolytic activity that generates p26, which is required to block eIF2α from phosphorylation.

The initiation of protein synthesis in mammals is the key regulatory step in mRNA translation and, thus, gene expression. Eukaryotic initiation factor 2 (eIF2) plays a central role in determining the rate of global protein synthesis (*1*). The latter step is regulated at the level of phosphorylation of the smallest α-subunit of eIF2, and the phosphorylation of eIF2α[1] is modulated by a cellular glycoprotein, p67, that is copurified with eIF2 (*2*). p67 binds to both the α- and γ-subunits of eIF2 (*3*, *4*). Since the discovery of p67 from rabbit reticulocytes and its functional characterization as a protector of eIF2α phosphorylation from kinases (*3*−*17*), there are numerous reports for the cloning and characterization of the p67 gene from different organisms (*18*−*24*).

Rat p67 is 480 amino acid residues long (*23*). This sequence can be divided into two major fragments: the N-terminal fragment of amino acid residues 1−107 (p26) and the downstream fragment of amino acid residues 108−480 (p52). In the p26 segment, there are two lysine-rich domains (I and II), which are separated by an acidic residue-rich domain (*6*). The lysine-rich domains are involved in the protection of eIF2α phosphorylation (*25*), and the acidic residue-rich domain negatively regulates the activity of the lysine-rich domains (*12*). In addition to the unique domains mentioned above, several serine/threonine clusters are also present at the N-terminus of p67, and one such motif ($_{60}$-SGTS$_{63}$) is modified by O-GlcNAcylation. This modification plays an important role in p67's stability and its association with the α-subunit of eIF2 and thus leads to the regulation of protection of eIF2α from phosphorylation by kinases (*26*).

At the p52 segment of p67, there is a consensus sequence ^{251}D(X)$_{10}$^{262}D(X)$_{68}$^{331}H(X)$_{32}$^{364}E(X)$_{94}$^{459}E^{460}H (ref *6* and references therein and ref *27*). These conserved amino acid

† Kent State University's Research Council supports this work.

* To whom correspondence should be addressed. Phone: (330) 672-3304. Fax: (330) 672-3816. E-mail: bdatta@kent.edu.

[1] Abbreviations: p67, eukaryotic initiation factor 2-associated 67 kDa glycoprotein; eIF2α, α-subunit of eukaryotic initiation factor 2 (eIF2); HRI, heme-regulated inhibitor; p52, downstream segment of amino acids 108−480 of p67; p26, N-terminal segment of amino acids 1−107 of p67; D251A, p67 mutant that has alanine instead of aspartic acid at position 251; D262A, p67 mutant that has alanine instead of aspartic acid at position 262; H231E, p67 mutant that has glutamic acid instead of histidine at position 231; MetAPs, methionine aminopeptidases; SDS−PAGE, sodium dodecyl sulfate−polyacrylamide gel electrophoresis; EGFP, enhanced green fluorescence protein; Myc-tagged p67 or its mutants, full-length p67 or its sequences that were fused with MASMQKLISEEDL amino acid residues, respectively; His-tagged proteins, proteins fused with six histidine residues.

10.1021/bi061838n CCC: $37.00
Published on Web 02/21/2007

residues are also present in methionine aminopeptidases (MetAPs). All MetAPs share the above conserved sequence and are structurally similar to prolidase, aminopeptidase P, and creatinase; all are members of the serine protease family (*27*−*29*). In the three-dimensional structure, five conserved amino acid residues (D251, D262, H331, E364, and E459) arrange themselves to coordinate two Co^{2+} ions in vitro (*29*−*30*). In an in vitro assay, this Co^{2+} binding is required for the cleavage of the terminal methionine from the artificial Met-Gly-Met-Met substrate (*22*, *31*). Recently, the identity of the metal binding to the conserved amino acid residues became controversial (*32*). Some reports claim that the metal, which binds to MetAP1/MetAP2, is Zn^{2+} (*33*, *34*), and one report claims that the metal is Mn^{2+} instead of Co^{2+} (*35*). Our mutational analysis of these conserved amino acid residues shows that substitutions of alanine for D251, D262, E364, and E459 abolish the functions of the lysine-rich domains in the cell culture system (*12*), thus indicating the possible coordination between the negatively charged conserved acidic residues and the positively charged lysine-rich domains in vivo.

The most important commonality between MetAPs from lower to higher organisms is their intermolecular proteolytic activity. The sequence of the p52 segment of p67 is significantly identical to those of both MetAP1 and MetAP2 (*29*), and the amino acid sequence of MetAP2 is almost identical (>95% identical) to that of mammalian p67 (*6*, *27*). A recent report (*32*) indicates that purified MetAP2, when stored at 4 °C for several days, has its p26 segment removed and the residual portion of the molecule still has the ability to remove the terminal methionine from the artificial substrate, Met-Gly-Met-Met. In this study, we examined whether rat p67 purified from baculovirus-infected Sf21 insect cells can generate the p26 segment and whether the amino acid sequences present at the p26 fragment are required to protect eIF2α from phosphorylation. Our studies show that rat p67 has autoproteolytic activity that generates several peptide fragments. Among these fragments, p26 and p52 are most stable and the p26 fragment is required for the protection of eIF2α phosphorylation in vivo and in vitro.

MATERIALS AND METHODS

All chemicals used in this study were obtained from Sigma Chemicals (St. Louis, MO), Merck (Darmstadt, Germany), ICN Biomedicals, Inc. (Aurora, OH), Fisher Chemicals, or GIBCO-BRL (Rockville, MD). All enzymes used in this study were purchased from New England Biolabs (Beverly, MA). Molecular mass markers were purchased from Bio-Rad, and [γ-^{32}P]ATP was purchased from Amersham.

Expression of His-Tagged Proteins from Baculovirus-Infected Sf21 Insect Cells

Recombinant viruses were generated for p67, its truncated versions (p52 and p26), p67 mutants D251A, D262A, and H231E, and eIF2γ following protocols as recommended by the manufacturer (Clontech). Proteins were purified from infected Sf21 insect cells following the procedures described previously (*3*, *26*).

Protein Fractionation through Different Column Chromatographic Steps

Recombinant rat p67 was tagged with a six-His tag and expressed in Sf21 insect cells on a large scale. Expressed protein was then affinity purified through Ni^{2+}−NTA−agarose beads in one step. The purity was tested via Coomassie staining and Western blot analysis. This preparation was then used for subsequent chromatographic steps as described below.

Separation via Sephadex G-50. Sephadex beads (Amersham Biosciences) were preswollen in PSSIV containing 0.1 M KCl. Swollen beads were used to set up the column at 4 °C, and the flow rate was adjusted to 1 mL/min. If necessary, column beads were equilibrated with 4−5 column volumes of respective PSSIV buffer containing the appropriate KCl concentration. The dialyzed and concentrated protein sample (p67 or its mutants) was loaded on top of the beads in the column, and PSSIV buffer was immediately added to continue the flow without drying the beads. Different fractions were collected and either frozen or analyzed.

Separation via Diethylmethylaminoethyl-Cellulose (DE52). DE52 beads were purchased from Whatman and processed (acid wash and base wash) following the manufacturer's recommendation. Beads were then stored in PSSIV with 0.1 M KCl at 4 °C. Appropriate amounts of processed beads were taken to set up the column at 4 °C and equilibrated with the storage buffer by passing 4−5 column volumes of the loading buffer over them. The dialyzed protein sample (p67 or its mutants) was loaded into the column at a concentration ∼0.5−0.25 mg/mL, and the flow rate was adjusted to 1 mL/min. Once the sample had been loaded, 3−4 volumes of wash buffer (same as the loading buffer) was passed through the beads and the flow-through and wash fractions were collected for further analysis. After the wash, the appropriate buffer was passed through the beads to elute the bound proteins and the same volume of different fractions was collected.

Separation via Cellulose Phosphate (P11). P11 beads were purchased from Whatman and processed according to the manufacturer's recommendation. Processed beads were stored in 20 mM potassium phosphate buffer, KPB [20 mM potassium phosphate (pH 7.5), 10% glycerol, 1 mM EDTA, and 5 mM β-MSH], at 4 °C for further analysis. Subsequent steps, i.e., setting up the column, equilibration, loading of the sample, wash, collection of flow-through and the wash, and elution, were the same as described in the previous paragraph.

Site-Directed Mutagenesis

Site-directed mutagenesis reactions were carried out following Kunkel's procedures as described previously (*25*). In brief, the uracil template of wild-type rat p67 was used for the DNA polymerase reaction in the presence of a 5′GCATTGGGAGTGTA**TTC**TGCAGCACAGTTGTTG3′ primer to change the histidine codon (5′CAT3′) to a glutamic acid codon (5′GAA3′) as shown with the bold and underlined triplet cDNA sequence. After the mutation had been confirmed by cDNA sequencing, it was subcloned into the BacPak8 vector for its expression in Sf21 insect cells.

In Vitro Phosphorylation Assay

In vitro phosphorylation assays using various purified proteins such as eIF2($\alpha\beta\gamma$), p67, and its fragments (p52 and p26) were performed, and phosphoproteins were analyzed

via SDS−PAGE following the procedures described previously (*3*).

Antibodies

A monoclonal antibody specific for the His probe (Sc-8036) was purchased from Santa Cruz Biotechnology. A monoclonal antibody specific for 6XHis-G (catalog no. 46-1008) was purchased from Invitrogen, whereas monoclonal antibodies specific for c-Myc (catalog no. K6003-1) was purchased from BD Biosciences. A monospecific polyclonal anti-eIF2α(P) antibody was purchased from Research Genetics (Huntsville, AL) and Cell Signaling Technology (Beverly, MA). Goat polyclonal antibodies specific for eIF2α (Sc-7629) and HRI (Sc-21949) were obtained from Santa Cruz Biotechnology. A monoclonal antibody specific for α-actin was purchased from Sigma. These antibodies were used in Western blots following the procedures recommended by the manufacturers.

Cell Growth, Transient Transfection Assays, and Generation of Stable Cell Lines

C2C12 mouse myoblast (ATCC) cultures were maintained in growth medium as described previously (*36*). Cultures of C2C12 cells (50−60% confluent) were transfected with plasmids complexed with Superfect following protocols described by the manufacturer (Qiagen). Plasmids used for the transfection reactions were Myc-tagged full-length p67 or its fragments, p52 and p26, that were cloned into pCMV-Myc (Clontech). Forty-eight hours after transfection, cells were harvested and cell lysates prepared; 100 μg of the total cell extracts was used for immunoblots. Transfection experiments were carried out in duplicate, and the experiments were repeated three times with similar results. KRC-7 cells were grown and transfected with individual plasmid, and cells constitutively expressing either EGFP or EGFP fusions of p67 or its mutants were selected by treating cells with G418 following the procedures described previously (*25*, *36*).

Reverse Transcription Polymerase Chain Reaction (RT-PCR)

Stable rat tumor hepatoma (KRC-7) cell lines were grown; cells were harvested, and total RNA samples were isolated and RT-PCRs carried out using 2 μg of total RNA following similar procedures described previously (*26*). For the polymerase chain reactions, the forward primer (5′CCCAGTCCGCCCTGAGCAAA3′) is designed from the extreme C-terminus of EGFP and the reverse primer (5′CTCGGCCGTGCTGGAGGT3′) is designed from the N-terminus of p67. These reactions should generate a 206-nucleotide DNA fragment.

Immunoblotting and Analysis of eIF2α Phosphorylation in Cell Lysates

C2C12 myoblasts were transiently transfected with plasmids encoding interacting proteins using Superfect reagents (Qiagen) following the manufacturer's protocols. Forty-eight hours after the addition of the DNA−Superfect complex to cells, cells were harvested and cell lysates were prepared; 100 μg total protein samples were analyzed on 15% SDS−PAGE gels. The proteins from the gels were transferred to nitrocellulose filters and detected on Western blots using specific antibodies. In the same transiently transfected cell extracts, the levels of eIF2α(P) were measured by analyzing 100 μg total protein samples via SDS−PAGE followed by detection of proteins with monospecific polyclonal antibodies specific for eIF2α(P) and total eIF2α. These experiments were repeated three times with similar results.

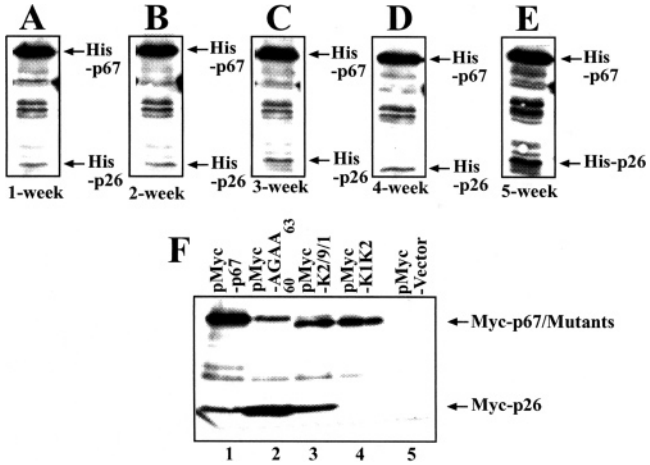

FIGURE 1: Time-dependent cleavage of p67. Rat recombinant p67 was purified from baculovirus-infected Sf21 insect cells. Purified samples were frozen in aliquots at −80 °C. At different time intervals (A−E), samples were thawed, and the proteins were denatured by boiling with SDS−PAGE loading buffer and analyzed on Western blots using a monoclonal antibody specific to the six histidine residues. (F) C2C12 cells were transiently transfected with the expression vector and the Myc-tagged p67 plasmid or plasmids carrying $_{60}$AGAA$_{63}$, K2/9/1, and K1K2 mutants of p67. Forty-eight hours after transfection, cells were harvested and lysates were prepared; 100 μg of total protein samples was analyzed via a Western blot using a monoclonal antibody specific to the Myc tag. Full-length Myc-tagged proteins are indicated as Myc-p67/mutants, and peptide fragment p26 is indicated as Myc-p26.

RESULTS

p67 Generates Several Peptide Fragments when Stored at −80 °C, and This Generation Is Time-Dependent. Purified proteins are reasonably stable when stored under appropriate temperature and buffer conditions. We therefore stored our purified p67 samples in several aliquots at −80 °C over a period of time. Each week, an aliquot of the p67 sample was thawed and analyzed by Western blot to detect its cleavage (Figure 1A−E). As clearly shown by the data, the extent of cleavage of p67 increases over time, and this cleavage generated a series of peptides that contain the N-terminal histidine tag. We further expressed in mammalian cells either wild-type p67 or its specific mutants, $_{60}$AGAA$_{63}$ (*26*), K2/9/1 (*25*), and K1K2 (*25*), that are tagged at their N-termini with the Myc epitope. These mutants were detected with a monoclonal antibody specific to the Myc tag on a Western blot (Figure 1F). The generation of several peptide fragments including p26 from wild-type p67 was very similar to that of His-tagged purified p67 (Figure 1A−E). However, the $_{60}$AGAA$_{63}$ mutant exhibited significantly increased levels of p26 as compared to either wild-type p67 or the K2/9/1 mutant (in Figure 1F, compare lane 2 with lanes 1 and 3). In contrast, the p26 fragment was completely undetected in the K1K2 mutant (Figure 1F, lane 4). In addition, the generation of the other peptide fragments was also affected by the mutations introduced into the p67 sequence (see the

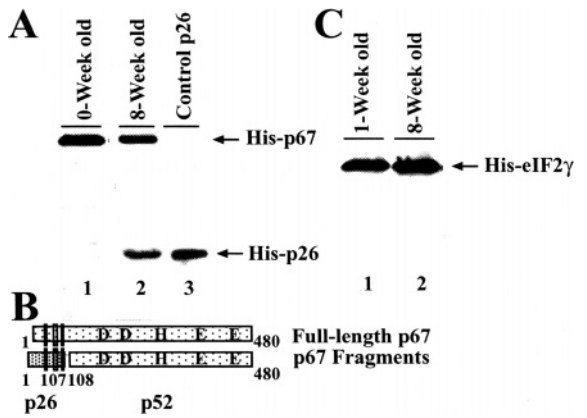

FIGURE 2: Recombinant rat p67, when stored at −80 °C, can generate the p26 segment of p67. A p67 sample purified from baculovirus-infected Sf21 insect cells was frozen at −80 °C for 8 weeks. After an initial storage, an aliquot of that sample (0.5 μg) was thawed and mixed with denaturing solution, boiled for 5 min, and analyzed on a 15% SDS−PAGE gel along with the freshly prepared sample of p67. Other samples included in that analyses were 0.25 μg of the His-tagged p26 segment of p67 that was also purified from baculovirus-infected Sf21 cells. Proteins were transferred to a nitrocellulose filter and probed with a monoclonal antibody specific to six histidine residues (A). A schematic diagram showing full-length p67 and its p26 segment and the downstream segment of amino acids 108−480, p52 (B). Identical procedures for purification from baculovirus-infected Sf21 insect cells, storage, and thawing were followed with eIF2γ. Samples of eIF2γ were analyzed in parallel with p67 samples, and proteins were detected via a Western blot using a monoclonal antibody specific to the His tag. The His tag is present at the N-terminus of p67 and its fragments and at the C-terminus of eIF2γ.

slower-migrating peptides in each mutant and compare those with wild-type p67). In parallel experiments, we purified p67 and its p52 and p26 fragments from baculovirus-infected Sf21 cells, and they eluted in different fractions that contained different amounts of proteins. These samples were then kept frozen at −80 °C for a period of 3 weeks. The fractions were then analyzed via SDS−PAGE gels and stained with Coomassie blue (Figure S1 of the Supporting Information). The fragmentation of full-length p67 was obvious (Figure S1A of the Supporting Information), whereas neither p52 (Figure S1B of the Supporting Information) nor p26 (Figure S1C of the Supporting Information) exhibited any detectable cleavage products, suggesting that both p26 and p52 fragments of p67 are the most stable fragments. This was further demonstrated by subsequent experiments (Figure 2) where we compared the fragmentation of freshly purified p67 (Figure 2A, lane 1) with an 8-week-old p67 aliquot (Figure 2A, lane 2) and purified p26 (Figure 2A, lane 3). In parallel experiments, we expressed, purified, and stored frozen a sample of His-tagged eIF2γ similarly as mentioned for rat p67. We then analyzed these samples side by side with p67 samples and detected them via a Western blot (Figure 2C). Our data show that p26 is quite stable even after storage for 8 weeks at −80 °C, and no other peptide fragments were detectable. Similarly, His-tagged eIF2γ was quite stable from the day it was purified.

The Degree of Fragmentation of p67 Is Increased at 0.75 M K^+. In our previous experiments, we used His-tagged p67 purified from baculovirus-infected Sf21 insect cells through an affinity column in one step. We used that purified sample and further fractionated it via molecular sieve chromatography using Sephadex G-50 (Figure S2), anion exchange chromatography using DEAE beads (Figure S3), and cation exchange chromatography using phosphocellulose beads (Figure S4). In all cases, we have also fractionated p67 using different concentrations of salts. A freshly prepared p67 sample exhibited a very low level of cleavage in the presence of 0.1 M KCl (Figure S2A), and the level of this cleavage was slightly increased when 1 M urea was supplemented with 0.1 M KCl (Figure S2B). p67 samples in 1 M urea and 0.1 M KCl, when stored frozen at −80 °C for 3 weeks, exhibited a significantly increased level of cleavage (Figure S2C). At 0.5 M KCl, the cleavage of p67 was minimal (Figure S2D); however, this cleavage was intensified in samples frozen for 3 weeks (Figure S2E). To our surprise, we noticed an extensive proteolysis of freshly purified p67 fractionated via Sephadex G-50 in the presence of 0.75 M KCl (Figure S2F), and the protein degradation led to the amino acid level when the sample was stored frozen for 3 weeks (Figure S2G). In the presence of 1 M KCl, the level of p67 cleavage was very low (Figure S2H) and did not increase significantly even in 3-week-old frozen samples (Figure S2I).

When a purified p67 sample was loaded into DEAE beads, a certain percentage of p67 was bound to the beads and the rest of it came in the flow-through (Figure S3, lanes 1−3). The bound population of p67 molecules started eluting at 0.5 M KCl (fractions 1−11), and almost all of it eluted at 0.75 M KCl (fractions 12−21). When p67 molecules started eluting in the presence of 0.75 M KCl, the level of cleavage of p67 increased and the cleavage patterns changed gradually (see fractions 14−16 in Figure S3A). The same fractions were analyzed after being stored for 3 weeks at −80 °C (Figure S3B,C), and we noticed very little cleavage on those samples that eluted in 0.5 M KCl (Figure S3B) and an extensive cleavage of p67 fractions that were eluted from the DEAE beads at 0.75 M KCl (Figure S3C).

When the purification procedure described above was followed with cation exchange beads like phosphocellulose, the cleavage of p67 was very minimal both in 20 mM KPB (Figure S4A, fractions 2 and 3, flow-through) and in 0.5 M KPB (fractions 1−9) and the level increased slightly when the protein was eluted with 0.75 M KBP (fractions 10−23). Although the p67 samples in 0.5 M KBP exhibited slight cleavage when stored frozen at −80 °C (Figure S4B), the level of proteolysis was remarkably high in p67 samples present in 0.75 M KBP that were stored frozen at −80 °C for 3 weeks (Figure S4C). Altogether, our data demonstrate that the level of p67 cleavage was higher when it is stored in buffer containing 0.75 M K^+, and this was intensified when the p67 sample was stored at −80 °C.

The D251A, D262A, and E364A Mutants of Rat p67 Exhibit Increased Stability that Correlates with Increased Levels of Endogenous p67. Five conserved amino acid residues (D251, D262, H331, E364, and E459) are present in the p52 segment of mammalian p67 (*6*). These residues coordinate with divalent metal ion and are involved in the proteolytic reaction to remove the terminal methionine from an artificial substrate Met-Gly-Met-Met (*22*). We wanted to test the notion that the conserved amino acid residues mentioned above may be involved in their proteolytic reaction as well. To test this idea, we constitutively expressed EGFP fusions of D251A, D262A, H331A, E364A, and

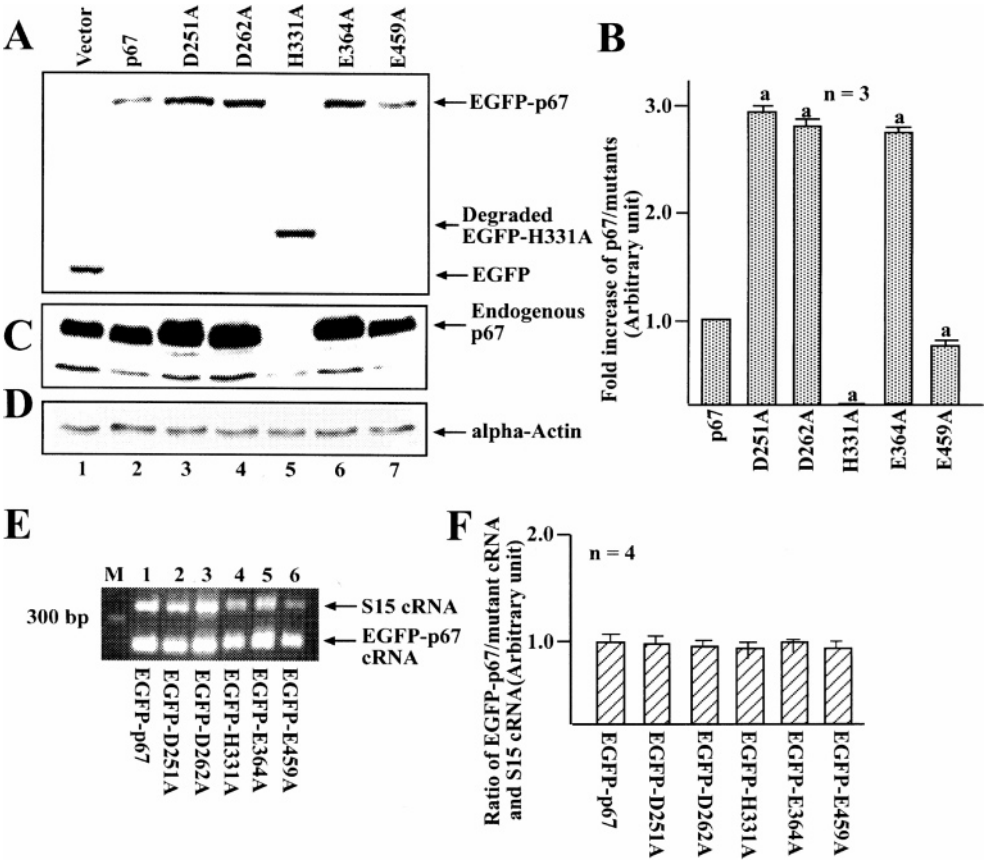

FIGURE 3: Stability of some of the p67 mutants at the protein level. Stable KRC-7 cells expressing either EGFP alone or its fusions with wild-type p67 and point mutants D251A, D262A, H331A, E364A, and E459A were grown in culture medium; cell lysates were prepared, and 100 μg of total proteins was analyzed on a 15% SDS−PAGE gel followed by Western blot analysis using a monoclonal antibody specific to EGFP (A). The band intensities were scanned, and the relative fold increase was calculated using NIH Image quant-162 (B). The results were from three different experiments. The data were analyzed using a one-way ANOVA, and the significance of the difference between wild-type p67 and p67 mutants was evaluated by a Student's *t*-test. *P* values of <0.05 were considered significant. The *P* values in case of a (vs p67) were <0.001 in all cases. The levels of endogenous p67 were measured in the cell extracts described above in a Western blot using a monospecific polyclonal antibody specific to p67 (C). As a control, the levels of α-actin were measured from the same cell extracts using equal amounts of total proteins (D). (E) Stable KRC-7 cells constitutively expressing EGFP fusions of either p67 or its point mutants D251A, D262A, H331A, E364A, and E459A were grown, and total RNA samples were isolated. RT-PCR was carried out using 2 μg of total RNA, and an equal amount of cRNA samples was analyzed on a 1.5% agarose gel. During PCR, primers for S15 mRNA were also used as an internal control. (F) The band intensities corresponding to S15 cRNA and EGFP-p67 cRNA were quantified using NIH Image quant-162, and the ratio of EGFP-p67 cRNA and S15 cRNA was calculated. This ratio was taken to be "1". The subsequent ratios from p67 mutants were normalized and plotted on a graph.

E459A mutants in rat tumor hepatoma cells and examined their levels of expression (Figure 3A,B). Surprisingly, we found that the levels of the D251A, D262A, and E364A mutants were at least 3-fold higher than the level of wild-type p67. In contrast, the level of the H331A mutant was significantly low and showed a degraded band migrating near 42 kDa (Figure 3A, lane 5). The level of the E459A mutant was very similar to the controls (compare lane 7 with lanes 1 and 2 in Figure 3A,B). In p67- and E459A mutant-expressing cells, the cleavage product (EGFP-p26) was very faint and could be detected only upon longer exposure of the blot (data not shown). In contrast, this EGFP-p26 fragment could not be detected in cells expressing D251A, D262A, and E364A mutants. This may be due to the mutation at the catalytic pocket that inhibited the cleavage. Our examination of the levels of endogenous p67 showed similar stability in the mutant-expressing cells mentioned above (Figure 3C). It is therefore conceivable that the cleavage of p67 is possibly mediated through dimer formation in mammalian cells. The increased levels of D251A, D262A, and E364A mutants could also be due to the presence of the increased levels of mRNAs in transfected cells. However, when we measured the level of mRNA by RT-PCR (Figure 3E) and quantified the EGFP fusion messages (Figure 3F), we noticed no change in the levels of mRNA from p67 and its different mutants. These results further support the notion that the accumulation of D251A, D262A, and D364A mutants in transfected cells is due to the inhibition of their autoproteolysis.

The D262A Mutant Exhibits a Decreased Level of Cleavage, whereas the H231E Mutant Shows an Increased Level of Autocleavage in Vitro. The increased stability of D251A, D262A, and E364A mutants in mammalian cells prompted us to test for their stability in vitro. We followed similar procedures to express and purify the mutants described above from baculovirus-infected Sf21 cells and fractionated via Sephadex G-50 beads in the presence of 0.1, 0.5, and 0.75 M KCl. The different fractions were collected from the columns and analyzed similarly as described in the legends of Figures S2−S4. The cleavage of the D262A mutant was significantly weaker at all three salt concentrations that were tested (Figure 4A−C). We have also tested the cleavage of

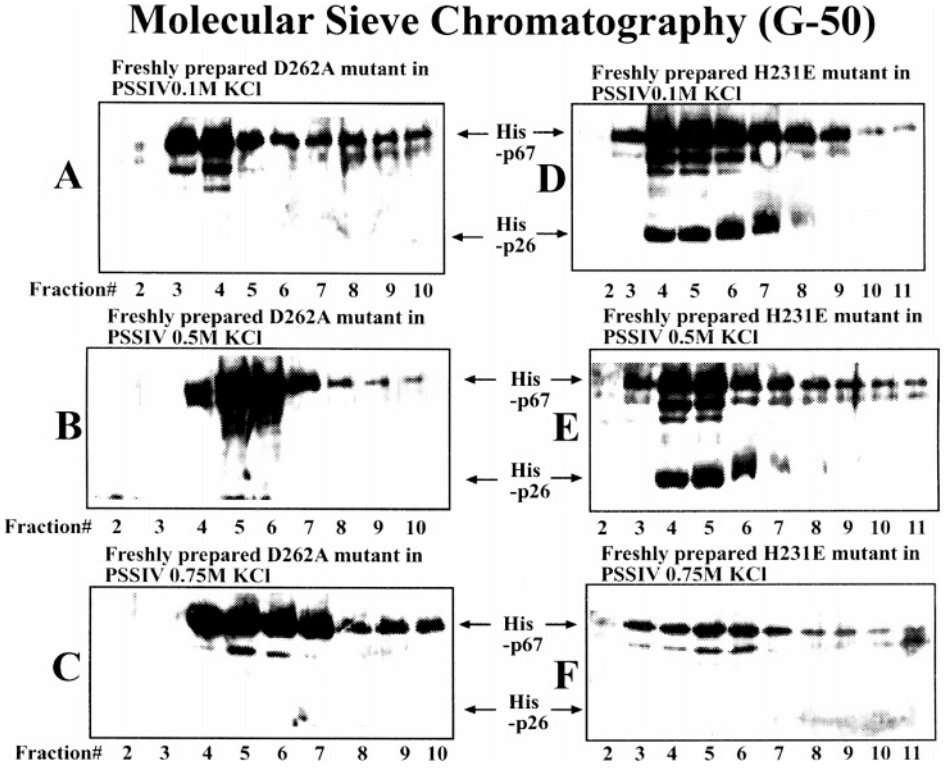

FIGURE 4: p67 mutant D262A that shows a reduced level of autoproteolytic activity with the H231E mutant showing an increased level of autoproteolysis. Both D262A and H231E mutants were expressed in baculovirus-infected Sf21 insect cells, affinity purified through Ni^{2+}−NTA−agarose beads, dialyzed in PSSIV containing 0.1 M KCl, and concentrated with Sephadex beads. Concentrated samples were then divided into three aliquots. The first aliquot was fractionated through G-50 equilibrated with PSSIV buffer containing 0.1 M KCl; 200 μL of each fraction was collected, 50 μL from each fraction analyzed on SDS−PAGE gels, and protein detected on a Western blot using a monospecific polyclonal antibody specific to p67 (A and D). The KCl concentration was adjusted to 0.5 M in the second aliquot, and similar analyses were performed as described for the first aliquot except the beads in the G-50 column were equilibrated with PSSIV containing 0.5 M KCl. The Western blot analyses of the proteins collected in different fractions are shown in panels B and E for the D262A and H231E mutants, respectively. Likewise, the KCl concentration was adjusted to 0.75 M in the third aliquot, and the sample was fractionated through a G-50 column equilibrated with PSSIV containing 0.75 M KCl following similar procedures as mentioned above. Proteins in different fractions were analyzed through Western blots similarly as mentioned above (C and F) for both D262A and H231E mutants.

the E364A mutant following similar procedures described above and found a cleavage pattern very similar to that of the D262A mutant (data not shown).

The H231 residue of MetAP2/p67 is known for its MetAP2 activity because an anti-angiogenic drug fumagillin binds to this molecule covalently in mammalian cells (*29*). Fumagillin binds to p67 in mammalian cells (*37*, *38*) and decreases its turnover rate (*39*). We therefore tested the cleavage of the H231E mutant in vitro. The H321E mutant was expressed and purified from baculovirus-infected Sf21 cells and fractionated via Sephadex G-50 in the presence of 0.1, 0.5, and 0.75 M KCl. An aliquot of fractionated samples was analyzed on a Western blot using p67 polyclonal antibodies and detected several peptide fragments in both 0.1 (Figure 4D) and 0.5 M KCl (Figure 4E). However, the level of this cleavage was significantly reduced in the presence of 0.75 M KCl (Figure 4F). In addition to the detection of the slower-migrating cleavage products, we also detected a faster-migrating peptide running around 26 kDa on SDS−PAGE gels, and it was confirmed to be p26 after further analyses (data not shown).

p52 Possibly Increases the Level of p67 Cleavage in Vitro, and This Cleavage Is Partially Inhibited by a Cocktail of Protease Inhibitors. The incubation of increasing amounts of p52 in reaction mixtures containing a fixed amount of full-length p67 at 37 °C for 1 h showed an increasing level of autoproteolysis of full-length p67 as compared to the wild-type molecule (in Figure 5A, compare lanes 3−6 with lane 1). Incubation of full-length p67 under identical conditions yielded at least two fragments, and their intensities increased when p67 was incubated with the p52 fragment. In addition to the increasing amounts of these two fragments (a and b, Figure 5B), a few more fragments appeared from p67 (Figure 5A, lanes 3−6). When we performed similar experiments with p52 alone (Figure 5C, lane 3), p26 alone (Figure 5C, lane 4), or their mixture (Figure 5C, lane 5) incubated at 37 °C for 9 h and examined the cleavage products, we noticed that p52 can generate only one cleavage product (lane 3, marked x), and this cleavage product disappeared when the p26 sample was added to the reaction mixture (lane 5). Analyses of both un-incubated samples of p52 (lane 1) and p26 (lane 2) revealed no cleavage products present within the samples prior to their incubation. These results suggest that both p52 and p26 fragments are quite stable, and the autocleavage of p52 is inhibited by p26. The proteolytic reactions mentioned here were conducted in the presence of 1 mM EDTA with no metal ion added. We performed similar experiments and added a serine protease inhibitor, PMSF, or a cocktail of protease inhibitors to the reaction mixture prior to the incubation at 37 °C for 1 h. We noticed that PMSF could not inhibit such cleavage, whereas a cocktail of protease inhibitors showed partial inhibition (compare lanes 5 and 6 in Figure 5D). Altogether, these data support the idea that p67 has intrinsic autoproteolysis activity.

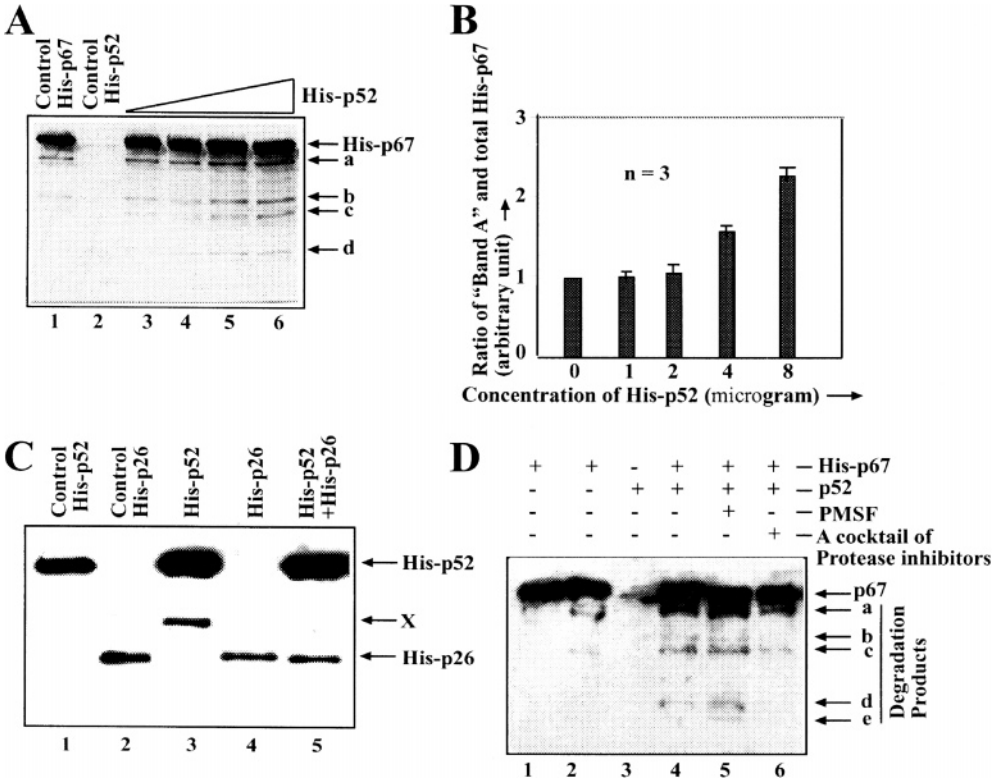

FIGURE 5: Autoproteolytic activity of full-length p67 which increased when p52 was added to it. A sample of purified p67 (0.5 μg) was mixed with increasing amounts of p52 (1, 2, 4, and 8 μg in lanes 3−6, respectively) and incubated at 37 °C for 45 min. The incubation buffer contains 25 mM Tris-HCl (pH 7.5), 5% glycerol, 5 mM EDTA, 2.5 mM β-mercaptoethanol, and 0.1 M KCl. As controls, an aliquot of p67 (0.5 μg, lane 1) or p52 (1 μg, lane 2) was also processed in parallel. The reactions were stopped with a denaturing solution and boiling for 5 min. The samples were analyzed on a 15% SDS−PAGE gel followed by detection of proteins using polyclonal antibodies specific to the p26 segment of p67 on Western blot. The polypeptide fragments are marked as a−d. The band intensities from a to d were scanned, and the ratios of band intensities with total His-p67 were calculated. These ratios for "band A" were most significant as compared to other bands. Therefore, only the ratios of "band A/His-p67" were plotted on a graph (B). Data from other bands are not shown. These results are from three independent experiments. (C) Freshly prepared p52 (0.5 μg, lane 1) and p26 (0.25 μg, lane 2) were incubated on ice, whereas 1 μg of p52 (lane 3), 0.125 μg of p26 (lane 4), and a mixture of p52 (1 μg) and p26 (0.125 μg) were incubated at 37 °C for 9 h. The samples were denatured with SDS loading buffer, boiled for 5 min, and analyzed on a 15% SDS−PAGE gel followed by detection of proteins on a Western blot using a monoclonal antibody specific to six histidines. The His-tagged proteins were labeled, and an autocleavage product of p52 is marked with an x. (D) The autoproteolytic activity of p67 could be partially inhibited by a cocktail of protease inhibitors. A freshly prepared sample of p67 (0.5 μg) from baculovirus-infected Sf21 insect cells was incubated with p52 (0.5 μg, lanes 4−6). To the reaction mixtures was added either 1.0 μg of PMSF (lane 5), or a cocktail of protease inhibitors (a mixture of bestatin, leupeptin, E64, AEBSF, and aprotinin) was added to the reaction mixture (lane 6). The same p67 sample alone was also incubated in the reaction mixture (lane 2). Likewise, 0.5 μg of p52 was also incubated alone in the reaction buffer (lane 3). An aliquot of a freshly prepared p67 sample was also analyzed in parallel without incubation at 37 °C (lane 1). After incubation of the reaction mixtures at 37 °C for 45 min, reactions were stopped by adding a denaturing solution and boiling for 5 min. The protein samples were analyzed on a 15% SDS−PAGE gel followed by detection of proteins with p67 antibodies on a Western blot. The peptide fragments (a−e) are marked. Fragment d seems to be the same as the p26 segment of p67. Lane 3 contains some overflow sample from lane 4.

The N-Terminal Fragment, p26, Is Required for the Protection of eIF2α Phosphorylation in Vivo. Our earlier experiments have demonstrated that p67 generates several peptide fragments in addition to the p26 fragment. Previously, we have reported that the unique domains such as lysine-rich domains I and II and the $_{60}$SGTS$_{63}$ motif are important for the protection of eIF2α from phosphorylation (*25*, *26*). We therefore wanted to test whether the p26 segment of p67 is required for the protection of eIF2α from phosphorylation in mammalian cells. When Myc-tagged full-length p67, p52, and p26 were expressed in mammalian cells in transient transfection assays, p67 lowered the levels of eIF2α phosphorylation by ∼75% (Figure 6A,C, lane 2), p52 had no effect (Figure 6A,C, lane 3), and p26 lowered it by more than 95% (Figure 6A,C, lane 4) as compared to mock transfected cells (lane 1). It is worthwhile to note that in addition to the expression of full-length exogenous p67, faster-migrating proteins, including the one migrating parallel to p26, were also detected only in cells expressing full-length p67 (Figure 6D, lane 2). These peptide fragments may have originated as a result of the autoproteolysis reaction. We also noticed a reciprocal relationship between the amounts of p26 present in the cells and the levels of eIF2α phosphorylation. Since we transfected C2C12 myoblasts with equal amounts of different plasmids expressing full-length p67 and its fragments, p52 and p26, the levels of expression of these proteins were very similar but their molar ratios are different. These results thus suggest that the p26 fragment of p67 is required for controlling the level of eIF2α(P) in C2C12 myoblasts.

The N-Terminal Fragment, p26, Has the Ability To Protect eIF2α from Phosphorylation in Vitro. To test for the function of p26 in in vitro phosphorylation assays, we phosphorylated a sample of eIF2 by a partially purified eIF2α-specific kinase, HRI (Figure 7A, lane 1). Prior to the addition of radiolabeled ATP to the reaction mixture, purified p67 (lane 2), p52 (lane

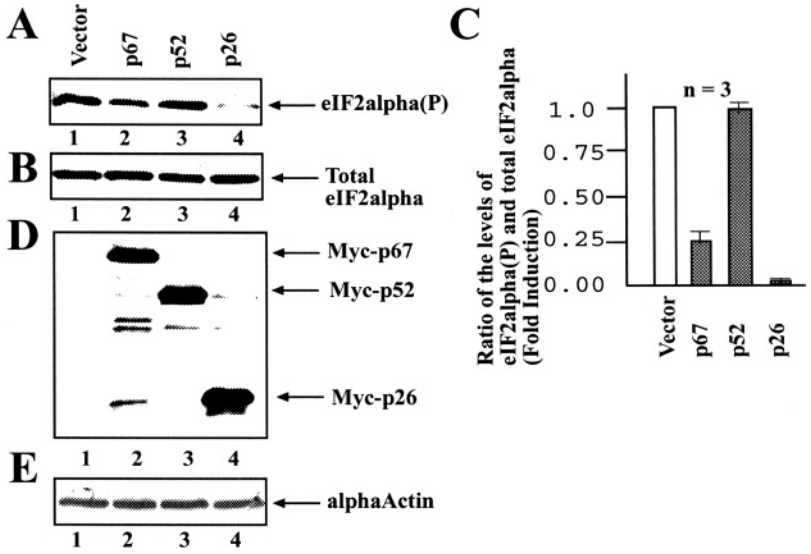

FIGURE 6: p26 segment of p67 that is sufficient for the protection of eIF2α phosphorylation activity in vivo. Expression plasmids carrying full-length p67, p52, and p26 which are fused in frame with a Myc tag at their N-termini were transiently transfected into C2C12 myoblasts; cell extracts were prepared 48 h after the addition of DNA precipitates to the cells, and 80 μg of total protein samples was analyzed on SDS−PAGE gels followed by detection of proteins on Western blots using a monospecific polyclonal antibody raised against eIF2α(P) for detection of the levels of the phosphorylated form of eIF2α(A). The levels of total eIF2α were measured from the cell extracts using monospecific polyclonal antibodies specific to the protein (B). The ratio of eIF2(P) to total eIF2α was determined from three independent experiments, and the results are plotted on a graph (C). The levels of the Myc-tagged proteins transiently expressed in C2C12 cells were analyzed on a Western blot using a monoclonal antibody specific to the Myc tag (D). As a control, the levels of α-actin were also measured in equal amounts of cell extracts (E).

3), and p26 (lane 4) were added. The phosphoproteins were analyzed on a SDS−PAGE gel followed by autoradiography (Figure 7A), and the phosphorylated form of eIF2α was further identified on a Western blot using monospecific antibodies to that form of eIF2α (Figure 7B). p67 exhibited strong protection of eIF2α phosphorylation activity; p52 had no effects, and p26 alone is sufficient for the protection of eIF2α phosphorylation catalyzed by HRI in vitro. In addition to the protection of eIF2α from phosphorylation, p26 may have activity that can inhibit the phosphorylation of HRI (Figure 7A, lane 4).

DISCUSSION

Numerous reports indicate that the p26 fragment of p67 is cleaved due to its autoproteolytic activity or due to the presence of the copurified contaminant protease(s) (*32*, *40*). When we look at the N-terminal amino acid sequence convergence between organisms, it is conceivable that the basic and acidic residue-rich domains are progressively added at the N-terminus of the molecule from lower organisms to mammals during evolution (*6*). These observations led us to test for a hypothesis that p67 has autoproteolytic activity that generates several peptide fragments along with p26, which is possibly required for the protection of eIF2α phosphorylation. Our data show that p67's autoproteolytic activity yields several peptides both in vitro and in vivo, and the amino acid sequences present in one such N-terminal peptide p26 are essential for p67's activity in protecting eIF2α from phosphorylation.

The generation of multiple peptide fragments from a protein could be due to the presence of a contaminant protease(s) or the fact that the protein has autoproteolytic activity. The source of the contaminant protease(s) could be specific to organisms, and different types of proteases will copurify with the protein. Since the different types of proteases have different specificities for cleaving after particular amino acid residues, the cleavage patterns of the protein will also be different (*41*, *42*). In this study, we have detected several His-tagged p67 fragments in both frozen samples that were purified from baculovirus-infected Sf21 insect cells (Figure 1A−E) and Myc-tagged fragments in transiently expressed rat p67 in C2C12 myoblasts (Figure 1F). In addition, a specific p67 mutant, $_{60}$AGAA$_{63}$, increases the generation of the p26 segment as compared to either-wild type p67 or the K2/9/1 mutant (Figure 1F), whereas the K1K2 mutant completely inhibited the generation of p26 in mouse C2C12 myoblasts (Figure 1F). This is consistent with our previous study, where we have shown that the $_{60}$-AGAA$_{63}$ mutant degrades rapidly and does not protect eIF2α from phosphorylation (*26*) and the K1K2 mutant cannot protect eIF2α from phosphorylation when it is constitutively expressed in rat KRC-7 cells (*25*). These results suggest specific cleavage of p67 in mammalian cells (rat and mouse), and irrespective of host cells expressing p67, the cleavage pattern is very similar. In addition, these results also indicate that the generation of several p67 fragments is not due to the presence of a contaminant protease(s). The finding that p26 and p52 segments of p67 are the most stable fragments further supports the latter conclusion (Figures S1 and 5), and these two fragments did not degrade either under frozen conditions (Figure S1) or after incubation for 9 h at 37 °C (Figure 5). His-tagged eIF2γ, when expressed, purified, and stored frozen following conditions identical to those for p67, did not exhibit any cleavage, indicating that no protease contaminant was copurified with eIF2γ under these conditions. These observations further support the fact that the contaminant protease(s) may not be present in p67 purified from baculovirus-infected insect cells. To prove this point in greater detail, we fractionated purified p67 via several column chromatographic steps (Figures S2−S4). p67's

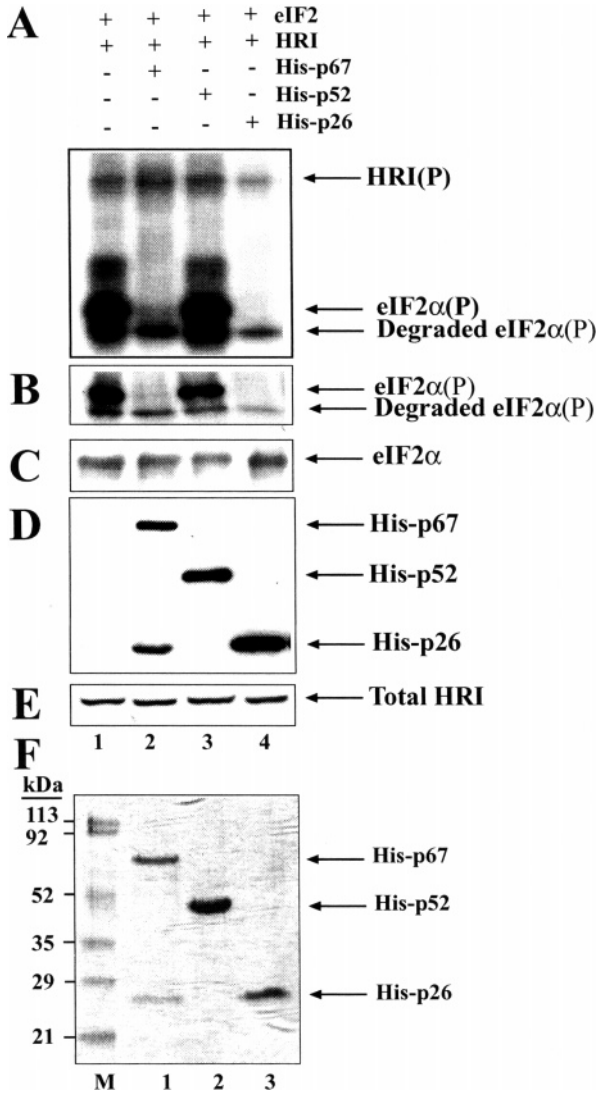

FIGURE 7: p26 segment of p67 that is sufficient for the protection of eIF2α phosphorylation activity in vitro. In in vitro phosphorylation assays, 2 μg of an eIF2 sample was incubated with HRI kinase alone (lane 1) or in the presence of 0.5 μg of His-p67 (lane 2), 0.75 μg of His-p52 (lane 3), or 1.5 μg of His-p26 (lane 4). The reactions were initiated by adding [γ-^{32}P]ATP and stopped by adding a denaturing solution and boiling for 5 min. The samples were analyzed on a 15% SDS−PAGE gel followed by detection of radiolabeled phosphoproteins via autoradiography (A) or transferred to nitrocellulose filters and detected by Western blots using polyclonal antibodies specific to the phosphorylated form of eIF2α (B), total eIF2α (C), a monoclonal antibody specific to a His tag (D), and polyclonal antibodies specific to total HRI (E). Protein samples of p67, p52, and p26 were analyzed on a 15% SDS−PAGE gel and stained with Coomassie blue (F). The p67 sample used in this experiment also contains the p26 segment (F, lane 2). Molecular mass markers are shown in lane M. Positions of the appropriate proteins are marked at right. The degraded eIF2α(P) peptide was identified by autoradiography (A) and Western blot analysis (B).

autocleavage was prominent under two conditions: (i) in the presence of 0.75 M K^+ and (ii) in frozen samples. Most proteases prefer to cleave their substrate by binding through protein−protein interactions, and this interaction is lost at higher salt concentrations or in the presence of a reagent such as urea that breaks hydrogen bonds (*42*). When fractionated p67 samples were exposed to either of the conditions, its level of cleavage was increasing (Figure S2B,F) rather than decreasing. In addition, the cleavage of p67 was detected in various fractions containing diluted samples of p67 obtained from different column chromatographic steps, further suggesting the autoproteolysis of p67 rather than cleavage mediated by the contaminant protease(s). The eluted p67 samples exhibited no or very little cleavage when these samples were freshly prepared but exhibited extensive cleavage when these samples were kept frozen at −80 °C (Figure S2). Altogether, our data suggest that the preparation of p67 from the Ni^{2+} affinity column does not contain protease contamination; rather, it cleaves due to autoproteolysis, and 0.75 M KCl is the optimal salt concentration for its cleavage in vitro. Although the latter salt concentration has no physiological meaning, it shows that in the presence of high salt p67 unfolds and this unfolding exposes the cleavage sites. During frozen conditions, the p26 portion of the molecule is possibly less dynamic and places itself on top of the catalytic core (p52 portion of the molecule). This possibly leads to the cleavage even at −80 °C. Our protein samples are always stored in buffer at pH 7.6. In our previous report (*8*), we have shown the existence of salt bridges between positively charged lysine ($pK_a \sim 10.1$) residues with the negatively charged aspartic/glutamic acid ($pK_a \sim 4$) residues. On the basis of the results shown here, we believe that 0.75 M KCl is causing the opening of the salt bridges and allowing the acidic residue-rich sequences to participate with the autoproteolytic cleavages of p67. Urea, which can break H-bonding interactions (*42*), is possibly doing the same thing. We have also tested the degradation of rat p67 at different pHs and found that it is degraded into the amino acid level at pH 4.0 (data not shown). At this pH, the N-terminal lysine residues in lysine residue-rich domains I and II and the acidic residues at the acidic domain are protonated and possibly do not favor the formation of salt bridges. This leaves the N-terminus free for coordination with the conserved amino acid residues at the downstream p52 segment of the molecules, and this leads to the rapid autoproteolysis.

The p52 segment of p67 has the appropriate motif, $^{251}D(X)_{10}{}^{262}D(X)_{68}{}^{331}H(X)_{32}{}^{364}E(X)_{94}{}^{459}E{}^{460}H$, that is present in MetAPs and is involved in proteolysis reactions (*6*, *40*). A published report (*40*) also suggests that the p52 segment alone can remove the methionine from the artificial substrate, Met-Gly-Met-Met, due to its proteolytic activity. The p52 segment also cleaves itself when incubated for long periods of time at 37 °C (Figure 5C). The level of cleavage of p67 was increased slightly when p52 was added to it (Figure 5A), and this cleavage was partially inhibited by a cocktail of protease inhibitors (Figure 5D) but not by PMSF, which can inhibit serine proteases (*41*). It is therefore clear that p67's autocleavage is not a serine protease type of cleavage. In addition to the evidence given above that purified p67 does not contain any protease contamination, we further demonstrated this idea by expressing and purifying some of p67's point mutants (Figure 4) with the notion that specific mutation at the enzymatic active site(s) may stop the autoproteolysis but not the cleavage mediated by the contaminant proteases. The D251A, D262A, and E364A mutants exhibited stability in mammalian cells; the H331A mutant was highly unstable, and the E459A mutant had no effect on its stability. In addition, the stability of endogenous p67 correlated with the stability of the mutants given above (Figure 3), indicating that the free form of p67 has the ability

to form dimer, which is active in autoproteolysis. When inactive mutants form the heterodimer with wild-type p67, the cleavage of both forms of molecules will also be inhibited. The amino acid residues given above are part of the active site for proteolytic reactions in MetAPs from several organisms (*29*). Our in vitro fractionation studies also support the notion given above. In this study, we notice that the H231E mutant exhibited hyperactivity toward autoproteolysis (Figure 4) and yielded large amounts of the p26 segment. The H231 site has been implicated as the substrate-binding site because an anti-angiogenic drug, fumagillin, binds to this site and inhibits MetAP2/p67 activity to cleave methionine from an artificial substrate, Met-Gly-Met-Met (*22*). In addition, binding of fumagillin to p67 decreases its turnover rate (*39*), supporting the notion that H231 is the active site for the autoproteolytic activity. Site-specific changes from histidine to glutamic acid at position 231 caused hyperactivity toward autoproteolysis (Figure 4). We believe that at pH 7.6, the NH group of the imidazole ring of histidine 231 is a weaker nucleophile because the pK_a of this group is 10.1. In contrast, the pK_a of glutamic acid is 4.0, and at pH 7.6, the carboxylate group of the glutamate side chain is a strong nucleophile. This provides a hyperactive catalytic center rather than inhibiting p67's autoproteolysis. We are now generating all possible H231 mutants to test for their autoproteolysis and provide evidence for the hypothesis given above.

Our mutational studies provide evidence that the basic lysine residue-rich sequences can form salt bridges with the conserved acidic residues (D251, D262, E364, and E459) but not with the conserved basic H331 residue (*8*, *12*). This coordination between the conserved acidic residues and the negatively charged N-terminal lysine residue-rich sequences will put the lysine residue-rich sequences close to the catalytic site that will facilitate the cleavage that generates the p26 segment. It is therefore conceivable that any protein that binds to the p52 segment will mask p67's autoproteolytic activity. Therefore, p67's binding to extracellular signal-regulated kinases (ERKs) at its p52 segment (*39*) will possibly block p67's autoproteolytic activity, and the p26 segment could be used to inhibit the activity of ERKs. Likewise, the binding of eIF2γ at the p52 segment possibly blocks its proteolytic activity and the binding at lysine residue-rich domain II to properly orient the active motifs, lysine residue-rich domain I and O-GlcNAcylation site, $_{60}$SGTS$_{63}$, into the negatively charged cavity (between the OB domain and the helical domains) of eIF2α (*43*) to mask serine 51. The O-linked GlcNAc moiety at the $_{60}$SGTS$_{63}$ motif may provide H-bonding interactions with the hydroxyl group of serine 51 and blocks eIF2α phosphorylation from its specific kinases.

ACKNOWLEDGMENT

We thank Professor Williams Merrick (Case Western Reserve University, Cleveland, OH) for his generous gift of the purified eIF2 sample.

SUPPORTING INFORMATION AVAILABLE

Coomassie staining of an aliquot of aged samples of p67, p52, and p26 (Figure S1), autoproteolytic cleavage of p67 that persists even after separation via molecular sieve chromatography (Figure S2), autoproteolytic cleavage of p67 copurified even after separation via anion exchange chromatography (Figure S3), and autoproteolytic cleavage of p67 that continues even after separation via cation exchange chromatography (Figure S4). This material is available free of charge via the Internet at http://pubs.acs.org.

REFERENCES

1. Merrick, W. C., and Hershey, J. W. B. (2000) Pathway and mechanism of initiation of protein synthesis, in *Translational control in gene expression* (Hershey, J. W. B., Mathews, M. B., and Sonenberg, N., Eds.) pp 33−88, Cold Spring Harbor Laboratory Press, Plainview, NY.
2. Datta, B., Chakrabarti, D., Roy, A. L., and Gupta, N. K. (1988) Roles of a 67 kDa polypeptide in protein synthesis inhibition in heme-deficient reticulocyte lysates, *Proc. Natl. Acad. Sci. U.S.A. 85*, 3324−3328.
3. Ghosh, A., Datta, R., Majumdar, A., Bhattacharya, M., and Datta, B. (2006) The N-terminal lysine residue-rich domain II and the 340−430 amino acid segment of eukaryotic initiation factor 2-associated glycoprotein p67 are the binding sites for the γ-subunit of eIF2, *Exp. Cell Res. 312*, 3184−3203.
4. Ray, M. K., Chakraborty, A., Datta, B., Chattopadyay, A., Saha, D., Bose, A., Kinzy, T. G., Hileman, R. E., Merrick, W. C., and Gupta, N. K. (1993) Characterization of the eukaryotic initiation factor 2 associated 67-kDa polypeptide, *Biochemistry 32*, 5151−5159.
5. Bose, A., Saha, D., and Gupta, N. K. (1997) Viral infection: I. Regulation of protein synthesis during vaccinia viral infection of animal cells, *Arch. Biochem. Biophys. 342*, 362−372.
6. Datta, B. (2000) MAPs and POEP of the roads from prokaryotic to eukaryotic kingdoms, *Biochimie 82*, 95−107.
7. Datta, B., Datta, R., Ghosh, A., and Majumdar, A. (2004) Eukaryotic initiation factor 2-associated glycoprotein, p67, shows differential effects on the activity of certain kinases during serum-starved conditions, *Arch. Biochem. Biophys. 427*, 68−78.
8. Datta, B., Datta, R., Ghosh, A., and Majumdar, A. (2006) The binding between p67 and eukaryotic initiation factor 2 plays important roles in the protection of eIF2α from phosphorylation by kinases, *Arch. Biochem. Biophys. 452*, 138−148.
9. Datta, B., Datta, R., Mukherjee, S., and Zhang, Z. (1999) Increased phosphorylation of eukaryotic initiation factor 2α at the G_2/M boundary in human osteosarcoma cells correlates with deglycosylation of p67 and a decreased rate of protein synthesis, *Exp. Cell Res. 250*, 223−230.
10. Datta, B., Ray, M. K., Chakrabarti, D., Wylie, D. E., and Gupta, N. K. (1989) Glycosylation of eukaryotic peptide chain initiation factor 2 (eIF-2)-associated 67-kDa polypeptide (p^{67}) and its possible role in the inhibition of eIF-2 kinase-catalyzed phosphorylation of the eIF-2α-subunit, *J. Biol. Chem. 264*, 20620−20624.
11. Datta, B., Ray, M. K., Chakrabarti, D., and Gupta, N. K. (1988) Roles of eIF-2 and eIF-2-associated protein in regulation of protein synthesis during growth of animal cells in culture, *Indian J. Biochem. Biophys. 25*, 478−482.
12. Datta, R., Tammali, R., and Datta, B. (2003) Negative regulation of the protection of eIF2α phosphorylation activity by a unique acidic domain present at the N-terminus of p67, *Exp. Cell Res. 283*, 237−246.
13. Gupta, S., Bose, A., Chatterjee, N., Saha, D., Wu, S., and Gupta, N. K. (1997) p67 transcription regulates translation in serum-starved and mitogen-activated KRC-7 cells, *J. Biol. Chem. 272*, 12699−12704.
14. Gupta, S., Wu, S., Chatterjee, N., Ilan, J., Ilan, J., Osterman, J. C., and Gupta, N. K. (1995) Regulation of a eukaryotic initiation factor-2 (eIF-2) associated 67-kDa glycoprotein (p^{67}) and its requirement in protein synthesis, *Gene Expression 5*, 113−122.
15. Ray, M. K., Datta, B., Chakrabarti, A., Chattopadhyay, A., Meza-Keuthan, S., and Gupta, N. K. (1992) The eukaryotic initiation factor 2-associated 67-kDa polypeptide (p67) plays a critical role in regulation of protein synthesis initiation in animal cells, *Proc. Natl. Acad. Sci. U.S.A. 89*, 539−543.
16. Saha, D., Wu, S., Bose, A., Chatterjee, N., Chakraborty, A., Chatterjee, M., and Gupta, N. K. (1997) Viral infection: II. Hemin induces overexpression of p67 as it partially prevents appearance of an active p67-deglycosylase in baculovirus-infected insect cells, *Arch. Biochem. Biophys. 342*, 373−382.

17. Wu, S., Rehemtulla, A., Gupta, N. K., and Kaufman, R. J. (1996) A eukaryotic translational initiation factor 2-associated 67 kDa glycoprotein partially reverses protein synthesis initiation by activated double-stranded RNA-dependent protein kinase in intact cells, *Biochemistry 35*, 8275−8280.
18. Cutforth, T., and Gaul, U. A. (1999) Methionine aminopaptidase and putative regulator of translation initiation is required for cell growth and patterning in *Drosophila*, *Mech. Dev. 82*, 23−28.
19. Klinkenberg, M., Ling, C., and Chang, Y. H. (1997) A dominant negative mutation in *Saccharomyces cerevisiae* methionine aminopeptidase-1 affects catalysis and interferes with the function of methionine aminopeptidase-2, *Arch. Biochem. Biophys. 347*, 193−200.
20. Kwon, J.-Y., Jeong, H. W., Kim, H. K., Kang, K. H., Chang, Y. H., Bae, K. S., Choi, J. D., Lee, U. C., Son, K. H., and Kwon, B. M. (2000) *cis*-Fumagillin, a new methionine aminopeptidase (type 2) inhibitor produced by *penicillium* sp. F2757, *J. Antibiot. 53*, 799−806.
21. Li, X., and Chang, Y. H. (1995) Molecular cloning of a human complementary DNA encoding an initiation factor 2-associated protein (p^{67}), *Biochim. Biophys. Acta 1260*, 333−336.
22. Li, X., and Chang, Y. H. (1995) Amino-terminal protein processing in *Saccharomyces cerevisiae* is an essential function that requires two distinct methionine aminopeptidases, *Proc. Natl. Acad. Sci. U.S.A. 92*, 2357−2361.
23. Wu, S., Gupta, S., Chatterjee, N., Hileman, R. E., Kinzy, T. G., Denslow, N. D., Merrick, W. C., Chakrabarti, D., Osterman, J. C., and Gupta, N. K. (1993) Cloning and characterization of complementary DNA encoding the eukaryotic initiation factor 2-associated 67-kDa protein (p^{67}), *J. Biol. Chem. 268*, 10796−10801.
24. Zhang, P., Nicholson, D. E., Bujnicki, J. M., Su, X., Brendle, J. J., Fredig, M., Kyle, D. E., Milhous, W. K., and Chiang, P. K. (2002) Angiogenesis inhibitors specific for methionine aminopeptidase 2 as drugs for malaria and leishmaniasis, *J. Biomed. Sci. 9*, 34−40.
25. Datta, R., Choudhury, P., Bhattacharya, M., Leon, F. S., Zhou, Y., and Datta, B. (2001) Protection of translation initiation factor eIF2 phosphorylation correlates with eIF2-associated glycoprotein p67 levels and requires the lysine-rich domain I of p67, *Biochimie 83*, 919−931.
26. Datta, R., Choudhury, P., Ghosh, A., and Datta, B. (2003) A glycosylation site, $_{60}SGTS_{63}$ of p67 is required for its ability to regulate the phosphorylation and activity of eukaryotic initiation factor 2α, *Biochemistry 42*, 5453−5460.
27. Bazan, J. F., Weaver, L. H., Roderick, S. L., Huber, R., and Matthews, B. W. (1993) Sequence and structure comparison suggest that methionine aminopeptidase, prolidase, aminopeptidase P, and creatinase share a common fold, *Proc. Natl. Acad. Sci. U.S.A. 91*, 2473−2477.
28. Keeling, P. J., and Doolittle, W. F. (1996) Methionine aminopeptidase-1: The MAP of the mitochondrion? *Trends Biochem. Sci. 21*, 285−286.
29. Liu, S., Widom, J., Kemp, C. W., Crews, C. M., and Clardy, J. (1998) Structure of human methionine aminopeptidase-2 complexed with fumagillin, *Science 282*, 1324−1327.
30. Arfin, S. M., Kendall, R. L., Hall, L., Weaver, L. H., Stewart, A. E., Matthews, B. W., and Bradshaw, R. A. (1995) Eukaryotic methionyl aminopeptidases: Two classes of cobalt-dependent enzymes, *Proc. Natl. Acad. Sci. U.S.A. 92*, 7714−7718.
31. Zuo, S., Guo, Q., Ling, C., and Chang, Y. H. (1995) Evidence that two zinc fingers in the methionine aminopeptidase from *Saccharomyces cerevisiae* is important for normal growth, *Mol. Gen. Genet. 246*, 247−253.
32. Yang, G., Kirkpatrick, R. B., Ho, T., Zhang, G.-F., Liang, P.-H., Johanson, K. O., Casper, D. J., Doyle, M. L., Marino, J. P., Jr., Thompson, S. K., Chen, W., Tew, D. G., and Meek, T. D. (2001) Steady-state kinetic characterization of substrates and metal-ion specificities of the full-length and N-terminally truncated recombinant human methionine aminopeptidase (type 2), *Biochemistry 40*, 10645−10654.
33. Walker, K. W., and Bradshaw, R. A. (1998) Yeast methionine aminopeptidase I can utilize either Zn^{2+} or Co^{2+} as a cofactor: A case of mistaken identity? *Protein Sci. 7*, 2684−2687.
34. Walker, K. W., and Bradshaw, R. A. (1999) Yeast methionine aminopeptidase I. Alteration of substrate specificity by site-directed mutagenesis, *J. Biol. Chem. 274*, 13403−13409.
35. Wang, J., Sheppard, G. S., Lou, P., Kawai, M., Park, C., Egan, D. A., Schneider, A., Bouska, J., Lesniewski, R., and Henkin, J. (2003) Physiological relevant metal cofactor for methionine aminopeptidase 2 is manganese, *Biochemistry 42*, 5035−5042.
36. Datta, B., Datta, R., Ghosh, A., and Majumdar, A. (2004) The stability of eukaryotic initiation factor 2-associated glycoprotein, p67, and that inhibits the phosphorylation of extracellular signal-regulated kinases 1 and 2, *Exp. Cell Res. 303*, 174−182.
37. Griffith, E. C., Su, Z., Niwayama, S., Ramsay, C. A., Chang, Y.-W., Wu, Z., and Liu, J. O. (1997) Molecular recognition of angiogenesis inhibitors fumagillin and ovalicin by methionine aminopeptidase 2, *Proc. Natl. Acad. Sci. U.S.A. 95*, 15183−15188.
38. Griffith, E. C., Su, Z., Turk, B. E., Chen, S., Chang, Y. W., Wu, Z., Biemann, K., and Liu, J. O. (1997) Methionine aminopeptidase (type 2) is the common target for angiogenesis inihibitors AGM-14470 and ovalicin, *Chem. Biol. 4*, 461−471.
39. Datta, B., Datta, R., Majumdar, A., and Balusu, R. (2004) Treatment of cells with the angiogenic inhibitor fumagillin results in increased stability of eukaryotic initiation factor 2-associated glycoprotein, p67, and reduced phosphorylation of extracellular signal-regulated kinases 1 and 2, *Biochemistry 43*, 14821−14831.
40. Sakamoto, K. M., Kim, K. B., Kumagali, A., Mercurio, F., and Crews, C. M. (2001) Protacs: Chimeric molecules that target proteins to the Skp1-Cullin-F box complex for ubiquitination and degradation, *Proc. Natl. Acad. Sci. U.S.A. 98*, 8554−8559.
41. Neurath, H. (1999) Proteolytic enzymes, past and future, *Proc. Natl. Acad. Sci. U.S.A. 96*, 10962−10963.
42. Lampi, K. J., Amyx, K. K., Ahmann, P., and Steel, E. A. (2006) Deamidation in human lens βB2-crystallin destabilizes the dimer, *Biochemistry 45*, 3146−3153.
43. Nonato, M. C., Widom, J., and Clardy, J. (2002) Crystal structure of the N-terminal segment of human eukaryotic translation initiation factor 2α, *J. Biol. Chem. 277*, 17057−17061.

BI061838N